Received: 3 December 2021 | Revised: 11 July 2022 | Accepted: 13 July 2022

DOI: 10.1111/1462-2920.16137

RESEARCH PAPER

environmental microbiology sfam

Daily dynamics of contrasting spring algal blooms in Santa Monica Bay (central Southern California Bight)

Gerid A. Ollison[1] | **Sarah K. Hu**[2] | **Julie V. Hopper**[1] | **Brittany P. Stewart**[1] | **Jayme Smith**[3] | **Jennifer L. Beatty**[1] | **Laura K. Rink**[4] | **David A. Caron**[1]

[1]Department of Biological Sciences, University of Southern California, Los Angeles, California, USA

[2]Woods Hole Oceanographic Institution, Marine Chemistry and Geochemistry, Woods Hole, Massachusetts, USA

[3]Southern California Coastal Water Research Project, Costa Mesa, California, USA

[4]Heal the Bay Aquarium, Santa Monica, California, USA

Correspondence
Gerid A. Ollison, Department of Biological Sciences, University of Southern California, 3616 Trousdale Parkway, Los Angeles, CA 90089-0371, USA.
Email: gollison@usc.edu

Funding information
United States National Science Foundation, Grant/Award Number: 1136818

Abstract

Protistan algae (phytoplankton) dominate coastal upwelling ecosystems where they form massive blooms that support the world's most important fisheries and constitute an important sink for atmospheric CO_2. Bloom initiation is well understood, but the biotic and abiotic forces that shape short-term dynamics in community composition are still poorly characterized. Here, high-frequency (daily) changes in relative abundance dynamics of the metabolically active protistan community were followed via expressed 18S V4 rRNA genes (RNA) throughout two algal blooms during the spring of 2018 and 2019 in Santa Monica Bay (central Southern California Bight). A diatom bloom formed after wind-driven, nutrient upwelling events in both years, but different taxa dominated each year. Whereas diatoms bloomed following elevated nutrients and declined after depletion each year, a massive dinoflagellate bloom manifested under relatively low inorganic nitrogen conditions following diatom bloom senescence in 2019 but not 2018. Network analysis revealed associations between diatoms and cercozoan putative parasitic taxa and syndinean parasites during 2019 that may have influenced the demise of the diatoms, and the transition to a dinoflagellate-dominated bloom.

INTRODUCTION

Numerous studies have firmly established the role of marine protists as integral to primary production, heterotrophic processes and global biogeochemical cycling (Azam et al., 1983; Caron et al., 2012; Pomeroy, 1974; Worden et al., 2015). Photosynthetic protists conduct nearly half of all oceanic primary production and are particularly important in coastal upwelling regimes located on the eastern boundaries of oceans; the so-called 'new production factories of the global ocean' (Falkowski et al., 1998; Field et al., 1998). The rapid proliferation of algae (algal blooms) in upwelling regimes that outpaces mortality caused by viral lysis, parasitic infection, or grazing results in short food chains that support the world's most important fisheries, and may account for a disproportionate amount of export flux of atmospheric CO_2 to the deep ocean (Buesseler, 1998; Gutierrez-Rodriguez et al., 2018; Ryther, 1969; Smetacek, 1999).

Algal blooms in eastern boundary ecosystems are generally the result of wind-driven upwelling of new nutrients (Chavez & Messié, 2009; Kudela et al., 2005). The characteristic equatorward winds along the west coasts of continents result in the net offshore transport of surface water, and the upwelling of nutrient-laden water, fuelling rapid algal proliferation during seasons of sufficient sunlight (Capone & Hutchins, 2013; Chavez & Messié, 2009). The timing of blooms along the Southern California Bight Region – part of the California

Current upwelling regime – is fairly consistent such that blooms are especially pronounced in the spring months when the strongest wind-driven upwelling intersects with ample sunlight and shallow mixing in the euphotic zone (Checkley & Barth, 2009; Smith et al., 2018).

A generality based on the physiological responses of different algal taxonomic groups to abiotic environmental forcing factors indicates that diatom species tend to dominate under the high nutrient, cool, shallow turbulent mixing conditions resulting from upwelling along the California coast. Dinoflagellates, by contrast, are predicted under warm, stratified, nutrient-poor conditions that are typical in the summer (Margalef, 1978; Shipe et al., 2008; Smayda & Reynolds, 2001). However, variability within and from that generality are common, and the specific taxa that will dominate a particular bloom are difficult to predict solely on the basis of measurable abiotic parameters. This situation implies that other factors dictate the specific community composition of a spring bloom.

Trophic interactions (biotic factors) are increasingly acknowledged as working synergistically with abiotic factors to shape community structure. Predation and viral lysis influence community structure in ways that are not easily attributable to abiotic conditions (Kranzler et al., 2019; Suttle, 2007). The role of symbiosis is also not well understood but can have a demonstrable impact on community structure. For example, parasitic protists that kill their hosts and release hundreds of free-living zoospores (zoosporic parasites) are globally distributed and have been shown to be an important source of mortality and community succession of microbial eukaryotes (Chambouvet et al., 2008; Guillou et al., 2008; Kim et al., 2017; Lima-Mendez et al., 2015; Park et al., 2002; Scholz et al., 2016). Recognition and studies of the ecological significance of these biotic factors for controlling community composition in free-living plankton assemblages have been made possible in part by advances in molecular and computational biology.

High-throughput sequencing (HTS)-based studies have enabled previously unattainable taxonomic breadth and resolution in the study of free-living protistan communities (Berdjeb et al., 2018; de Vargas et al., 2015; Hu, Connell, et al., 2018). Daily measurements are especially appealing for understanding the factors controlling community composition and turnover of protists because one can account for both photosynthetic and heterotrophic community turnover on time scales that are relevant to growth and mortality processes (Field et al., 1998; Fuhrman et al., 2015). Moreover, recent applications of RNA-based (cDNA) HTS have been particularly instrumental in distinguishing metabolically active members of the community from senesced or dead cells, extracellular DNA, as well as reducing bias resulting from highly variable gene copy number in protists (Charvet et al., 2014; Gong & Marchetti, 2019; Hu et al., 2016; Massana et al., 2015; Ollison et al., 2021).

Robust sequence datasets generated in HTS studies are also amenable to networking analyses that can aid in the identification of trophic interactions among the many taxonomic units ('species' or 'strains'; OTUs or ASVs) generated by HTS studies (Faust & Raes, 2012; Layeghifard et al., 2017; Muller et al., 2018; Newman, 2004; Poulin, 2010; Proulx et al., 2005; Rottjers & Faust, 2018; Wang et al., 2017). Pairwise association calculation, such as Pearson's and Spearman's rank correlation coefficients have been widely adopted (Faust et al., 2015; Jones et al., 2018; Needham et al., 2017; Xia et al., 2011). Recent graphical lasso-based approaches assume sparsity in HTS datasets (most species pairs are assumed not to interact) and account for interdependence of species (compositional bias), while employing the concept of conditional independence; two nodes (i.e. species) in the graphical model are conditionally independent if they provide no information about the state of the other given the states of all other species in the dataset. As a result, each link produced by the model implies a direct connection, as opposed to correlated but indirectly connected ASVs (Friedman et al., 2007; Kurtz et al., 2015; Tackmann et al., 2019; Yoon et al., 2019).

In this study, changes in the protistan community and corresponding environmental conditions were tracked daily during two spring blooms in April 2018 and 2019 in Santa Monica Bay, California (Hickey, 1979, 1992). 18S rRNA gene transcript (RNA) sequencing and chemical/physical measurements were performed to examine the biotic and abiotic factors that may shape protistan community structure during the blooms.

EXPERIMENTAL PROCEDURES

Sample collection

Algal blooms along the coast in the Southern California Bight (SCB) region typically follow significant, seasonal upwelling events driven by episodic, seasonal equatorward (northerly) winds (Kim et al., 2009; Kudela et al., 2005; Kudela et al., 2010; Seubert et al., 2013). Blooms were targeted in Santa Monica Bay during spring 2018 and 2019 using local meteorological information to anticipate coastal upwelling events (Figure S1). Sampling from the Santa Monica Pier (SMP) was conducted daily at 0900 from the same location and orientation on the SMP from the 16 through the 30 in April 2018 (15 days), and in 2019 from the 13 April through 6 May (22 days; no sample was collected on the 14 April 2019). Sampling periods are henceforth referred to as 2018 and 2019, respectively.

An RBR Concerto (https://rbr-global.com) was deployed in surface water for 15 min at the time of each sample collection to obtain temperature, conductivity, chlorophyll *a* fluorescence, and dissolved oxygen concentrations (Table S1). A 20 μm mesh plankton net was drift towed from the pier (15 min), and samples examined via light microscopy to identify the dominant planktonic taxa and their relative abundances. Surface water was collected via bucket tosses from the pier and was used for 18SrRNA transcript sequencing, nutrient analyses, extracted chlorophyll concentrations, and domoic acid concentrations; an extended funnel was used to gently fill a single acid-washed-3x-rinsed 20 L carboy per established laboratory protocol (https://www.protocols.io/view/sample-collection-from-the-field-for-downstream-mo-hisb4ee). The carboy was protected from the light and immediately transported approximately 300 m to the Heal the Bay Aquarium located at the SMP for sample processing.

Sample processing

Microscopic determinations of dominant plankton was made from 90 ml samples of seawater preserved with 10 ml of acid Lugol's solution (1%) (Auinger et al., 2008), analysed following Utermöhl methodology (Utermohl, 1958) using a using a Leica DM IRBE inverted light microscope. Molecular community analyses were performed in triplicate on 2 L seawater samples pre-filtered with nitex mesh (80 μm) and collected on 45 mm GF/F filters (nominal pore size 0.7 μm, Whatman, International Ltd. Florham Park, NJ) to capture the unicellular eukaryote community while excluding most metazoa from the samples. The filters were placed in a 15 ml RNAse-free Falcon tube containing 1.5 ml of RLT buffer + betamercaptoethanol, immediately flash frozen in liquid nitrogen, and subsequently stored at −80°C until RNA extraction. Chlorophyll *a* (hereafter referred to as chlorophyll) was used as a proxy for biomass and bloom magnitude. Major blooms were categorized using two standard deviations (SD = 4.6) added to the 15-year average (~2.8 μg/L; 2008 through 2020, minus year 2015) at the SMP (Kim et al., 2009; Seubert et al., 2013). Extracted chlorophyll and particulate domoic acid concentrations (pDA in 2018 only) were determined by filtering up to 300 ml of seawater onto 25 mm GF/F filters in duplicate. Less than 300 ml of seawater was collected for chlorophyll samples in 2019 when the filters clogged during periods of high biomass. Filters collected for chlorophyll analysis were extracted in 100% acetone at −20°C in the dark for 24 h and then analysed fluorometrically via the non-acidification method using a Trilogy Turner Designs fluorometer. Samples collected for domoic acid quantification were analysed via Mercury Science, Inc., DA enzyme-linked immunosorbant assay (ELISA: Mercury Science, Durham, NC) according to the methods described in (Seubert et al., 2013). Samples for nitrite + nitrate and phosphate were measured from 0.02 μm filtered seawater via flow injection analysis on a Quickchem 8500 at the Marine Science Institute Analytical Lab, UCSB. Meteorological data were collected from NOAA buoy station 46025 (https://www.ndbc.noaa.gov/).

RNA extraction and sequencing

Total RNA was extracted per a previously established protocol (https://www.protocols.io/view/rna-and-optional-dna-extraction-from-environmental-hk3b4yn) (Ollison et al., 2021). Briefly, each GF/F filter was shredded by vortexing after the addition of silica beads to each tube containing a GF/F filter and lysis buffer. The mixture was transferred to a syringe that was used to obtain the lysate from the filter/water slurry. RNA was extracted from the lysate via Qiagen All Prep DNA/RNA Mini Kit (Qiagen, #80204) per manufacturer instructions. Genomic DNA was removed prior to RNA extraction using an RNase-Free Qiagen DNase (Qiagen, #79254). RNA was reverse transcribed to cDNA using the Bio-Rad iScript Reverse Transcription Supermix with random hexamers (Bio-RAD, #170-8840).

The 18S rRNA V4 region in each sample was PCR amplified using 18S 565F (5'-CCAGCASCYGCGGTAATTCC-3′) and 948R (5'-ACTTTCGTTCTTGATYRA-3′) primers (Stoeck et al., 2010) via Q5 High-Fidelity 2x Master Mix (NEB, #M0492S). PCR reactions were carried out in two steps due to the difference in annealing temperature between primer pairs. The PCR reaction consisted of an initial 98°C denaturation for 2 min, and 10 cycles of 98°C for 10 s, 53°C for 30 s, and 72°C for 30 s. The final 15 cycles consisted of 98°C for 10 s, 48°C for 30 s and 72°C for 30 s. A final extension at 72°C for 2 min was performed after both steps. PCR products were subsequently purified using Agencourt AMPure XP beads (Beckman Coulter #A63881), indexed using Illumina-specific P5 and P7 indices, quantified using a QuBit 2.0 fluorometer (ThermoFisher, #Q32866), and normalized to 10 μM prior to sequencing. Normalized samples were quality checked on an Agilent Bioanalyzer 2100 and paired-end sequenced (250 × 250) on an Illumina MiSeq (Laragen Inc. Culver City, CA).

Sequence analysis

ASV calling

18S rRNA V4 amplicon sequences were demultiplexed, quality filtered, denoised, merged, chimera checked, dereplicated, and grouped into amplicon sequence

variants (ASVs) via the DADA2 plugin of Qiime2 (v2020.11) (Bolyen et al., 2019). Barcodes, primers, and low-quality bases at the ends of both forward and reverse reads were assessed with the interactive quality plot and removed using the *trim* and *trunc* options of the DADA2 plugin (*--p-trim-left-f 12 --p-trim-left-r 12 --p-trunc-len-f 250 --p-trunc-len-r 250*). ASVs were assigned taxonomic classifications at 90% identity using the PR2 database (v12; Guillou et al., 2008) (Table S2).

ASVs occurring 50 times or less throughout the entire dataset were removed to attenuate background noise; sequences suspected of being contaminant sequence were removed using the decontam R package (Davis et al., 2018). Samples were subsequently normalized using the trimmed mean by M value method (edgeR) before further analysis (Robinson et al., 2010). Taxonomic identification was assigned at approximately phylum level for easier interpretation and manually assigned higher classification for diatom and dinoflagellate genera. UpSet plots were generated from TMM-normalized, binary ASV tables using the UpSetR package (Conway et al., 2017). A detection limit for ASV presence and absence was defined as ASVs with ≥10 reads in a sample were given a 1 for presence; those with <10 were assigned 0 for absence. The most abundant diatom and dinoflagellate ASVs were investigated by removing ASVs below a 1% cutoff score within their respective assemblage. The individual ASVs that accounted for ≥1% of total diatom or dinoflagellate reads were considered abundant ASVs in subsequent analyses. Abundant ASVs were aggregated at approximately genus level, and the dominant taxa, containing multiple ASVs, were those that accounted for 10% or more read abundance of the sampling period.

Community analysis

Inverse Simpson index was calculated in R using the diversity function (Vegan v2.4–2). Total species richness was estimated by tallying the number of unique ASVs (after the removal of singletons). Cluster dendrograms were generated by combining pairwise Euclidean distances with the average method of clustering. After quantifying Euclidean distances between individual samples, the pairwise averages were used as the distances between other samples, pairs and clusters.

Co-association networks for the 2018 and 2019 sampling periods were constructed using the SPIEC-EASI R package (Kurtz et al., 2015). SPIEC-EASI uses a centred log ratio transformation and a graphical lasso approach to identify direct associations between ASVs while simultaneously addressing the sparsity and composition bias inherent in all rRNA-based datasets (Kurtz et al., 2015). Nodes (also called *vertices*) represent ASVs, and links (also called *edges*) represent correlations (positive associations) and anti-correlations (negative associations) between ASVs. Links with a weight below |0.01| and all disconnected nodes were removed before down-stream analysis. Network structural properties (clustering coefficient, summary statistics of network degree and betweenness-centrality, network diameter, and average path length) were calculated using the igraph package (Csardi & Nepusz, 2005).

Raw sequence data can be found on NCBI SRA under project number PRJNA480318, and all R scripts used for data analysis can be found at https://github.com/theOlligist/Daily_dynamics-SMP.

RESULTS

Community responses to physical and chemical dynamics

Sampling was conducted for 15 and 22 consecutive days in Santa Monica Bay the spring of 2018 and 2019, respectively, to investigate protistan community dynamics associated with spring upwelling algal blooms. Short periods of elevated, down-coast (northerly) winds just prior to the initiation of sampling at the pier during these years were associated with lowered surface water temperatures and higher salinity values, characteristic of upwelled deep water in the region (Figure 1; Figure S1B,C). The lowest recorded surface water temperature during 2018 was 12.8°C on Day 3 with a concomitant rise in salinity that is characteristic of upwelled water in the region (Figure 1A). Temperature gradually warmed to approximately 16°C during the remainder of the sampling period while salinity decreased during the first 4 days following wind stress and then increased gradually for the remainder of the study period. Low surface water temperatures were less pronounced and more sporadic during 2019, with the lowest value (13.8°C) observed on Day 1 and modest minima also observed on Day 5 (14.5°C) and Day 10 (14.3°C), with a gradual increase to 16–17°C during the remainder of the sampling period (Figure 1B). Salinity increased on Day 4 during 2019 and remained relatively high until Day 11, decreased again Day 12–14, and then gradually increased again for the remainder of the sampling period. It is unclear if the variability was a consequence of weak wind events that occurred during the sampling period, the advective movement of water at the pier, or both (Figure 1B; Figure S1C).

Inorganic nutrient concentrations (nitrite + nitrate and phosphate) were elevated coincident with low temperatures and high salinity values observed at the beginning of each sampling period (Figures 1 and 2; Table S1). Nitrite + nitrate concentrations increased from approximately 3–10 μM during the first 3 days of sampling in 2018 and declined rapidly (Figure 2A;

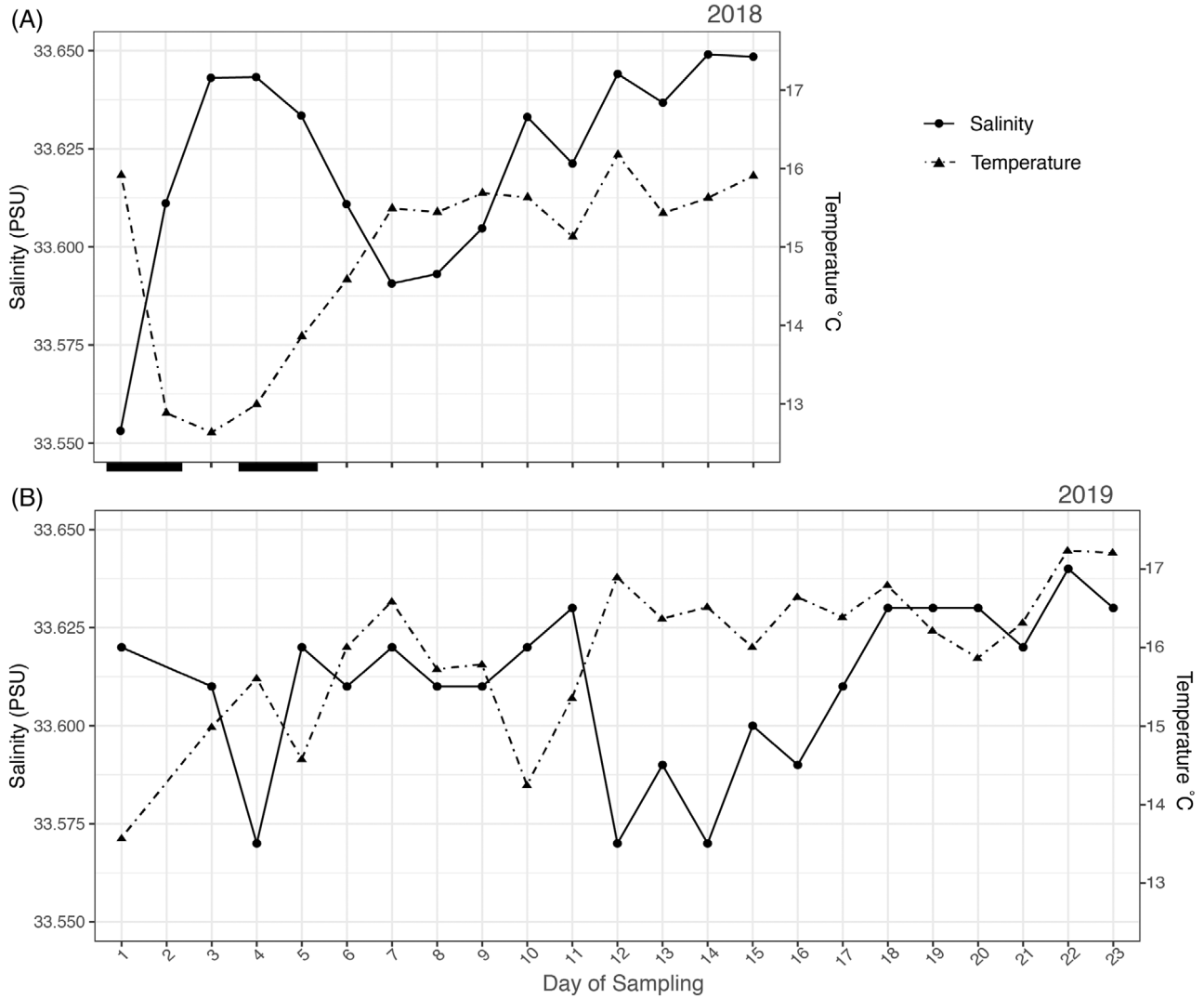

FIGURE 1 Temperature (triangles with dashed line) and salinity (filled circles with solid line) dynamics during 2018 (A) and 2019 (B) at the Santa Monica Pier. Black horizontal bars below graph A represent periods of relatively high amplitude winds. Sampling from the Santa Monica Pier (SMP) was conducted daily at 0900 from the same location and orientation on the SMP from the 16 through the 30 April 2018 (15 days), and in 2019 from the 13 April through 6 May (22 days; no sample was collected on the 14 April 2019)

Table S1). Nitrite + nitrate concentration was high on Day 1 during 2019 (8 μM) and declined rapidly to <1 μM between Day 1 and Day 4 (Figure 2B; Table S1). The latter finding implies that bloom initiation, and consequent nutrient drawdown, may have already begun by the time sampling began in 2019. Phosphate values were substantial at the beginning of the sampling periods in both years, and remained variable during the duration of each sampling period (Figure 2).

Extracted chlorophyll concentrations increased markedly on Day 5 during 2018, 2 days after maximal nitrite + nitrate concentration was observed, with a gradual decline for the remainder of the sampling period (Figure 2A; Table S1). Chlorophyll concentrations were generally higher in 2019 relative to 2018, but the initial response of chlorophyll (≈18 μg/L on Day 4) during 2019 was comparable to the maximal value observed on Day 5 during 2018. Beyond that day, however, chlorophyll values in 2019 remained relatively high throughout the sampling period, with exceptionally high concentrations observed between Day 16 and Day 21. This period of elevated chlorophyll values had a maximal concentration > 60 μg/L recorded on Day 18 (Figure 2B; Table S1). Blooms during both years were characterized as major blooms for the region according to chlorophyll concentration (see Experimental Procedures section).

Dominant taxa and community dynamics differed between 2018 and 2019

Daily changes in community composition and diversity of the metabolically active protistan community were

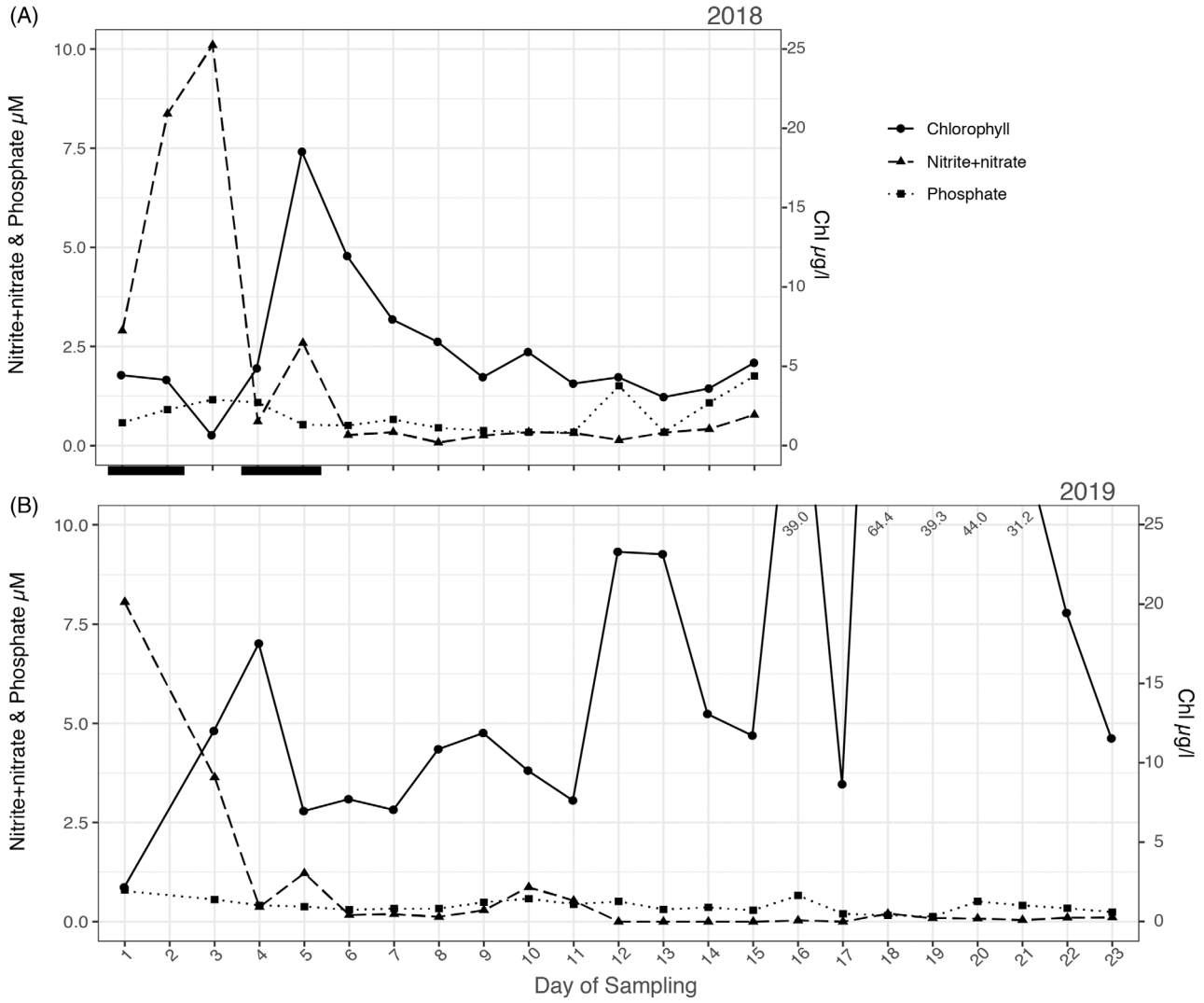

FIGURE 2 Concentrations of extracted chlorophyll (filled circles with solid line), nitrite + nitrate (triangle with dashed line), and phosphate (square with dotted line) during the 2018 (A) and 2019 (B) sampling periods at the Santa Monica Pier. Values larger than the figure scale on some sampling dates in B are shown at the top of the graph. Black horizontal bars below graph A represent periods of relatively high amplitude winds. Sampling from the Santa Monica Pier (SMP) was conducted daily at 0900 from the same location and orientation on the SMP from the 16 through the 30 April 2018 (15 days), and in 2019 from the 13 April through 6 May (22 days; no sample was collected on the 14 April 2019)

characterized by sequencing the V4 hypervariable region of 18S rRNA gene transcripts (RNA) during algal blooms in 2018 and 2019. A total 27,442,839 sequenced reads with an average of 241,975 sequences per sample formed 29,643 total ASVs. A total of 1102 ASVs remained after filtering of possible contaminant sequences and (rare) ASVs that accounted for ≤50 reads throughout the entire dataset. Large differences were observed between the 2 years in quantitative estimates of species richness, diversity, as well as taxonomic composition. Hierarchical clustering of all samples illustrated that Year (2018 vs. 2019) was the primary difference in community composition (among all 37 samples; Figure S2A). The exceptions were four samples taken before Day 7 in 2019 that clustered more closely with samples from 2018.

Diatoms were the most abundant taxa observed from Day 2 through Day 10 during 2018 (Figure 3A). Diatoms reached peak relative abundances on Days 4 and 5 in that year, and gradually declined over the remaining 10 days of sampling. Haptophytes and archaeplastids accounted for significant fractions of the phototrophic assemblage with relatively unchanging relative abundances throughout the sampling period in 2018. Cryptophytes and pelagophytes constituted minor components of the phytoplankton community throughout 2018, whereas dinoflagellate relative abundance was lower at the beginning of the study and gradually increased coincident with the decline of diatom relative abundance.

In contrast to 2018, dinoflagellates were consistently the dominant taxa during 2019, and accounted

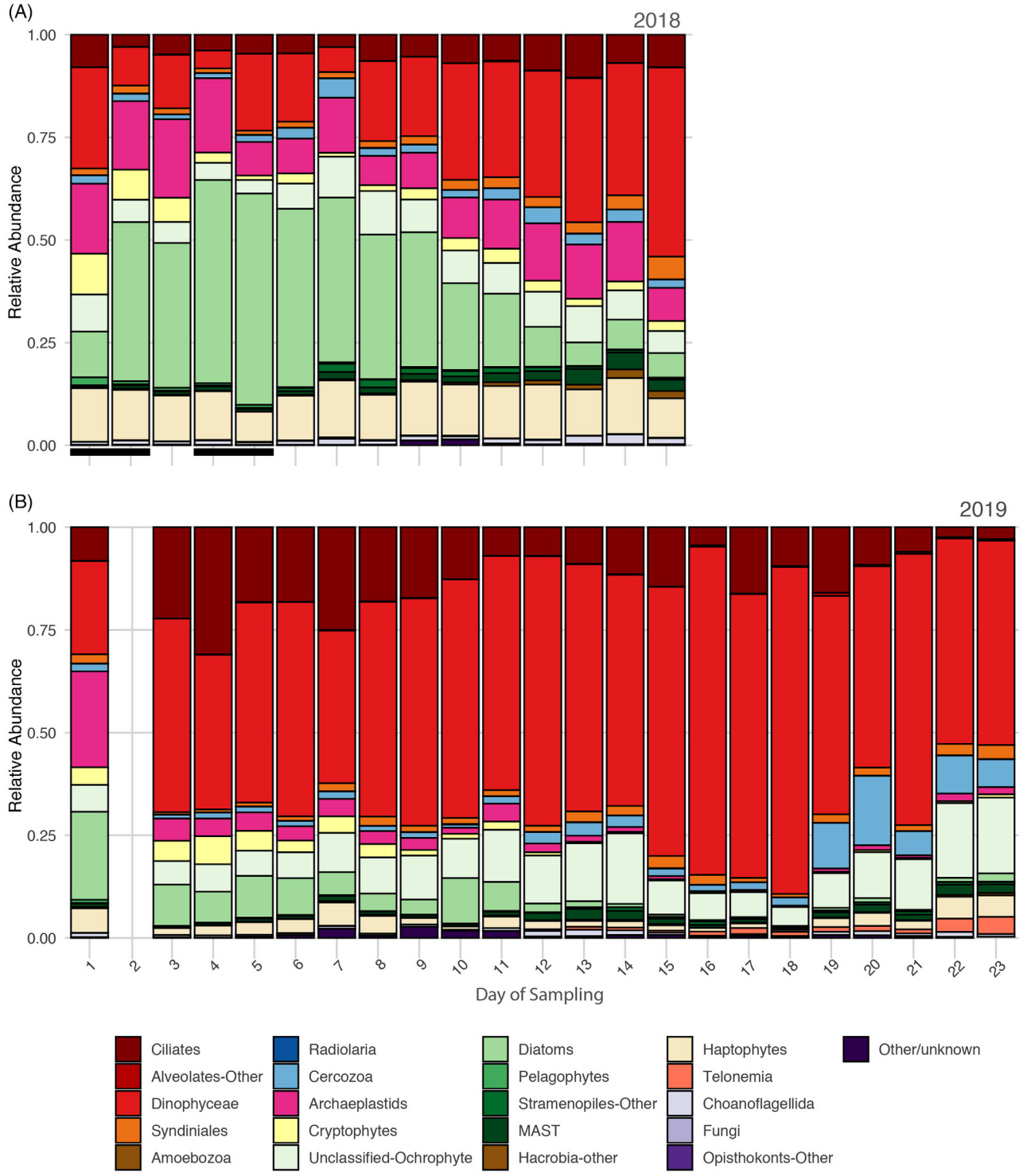

FIGURE 3 Changes in the relative proportion of major protistan taxonomic groupings during the sampling periods in 2018 (A) and 2019 (B). Black horizontal bars below figure a represent periods of relatively high amplitude winds. Sampling from the Santa Monica Pier (SMP) was conducted daily at 0900 from the same location and orientation on the SMP from the 16 through the 30 in April 2018 (15 days), and in 2019 from the 13 April through 6 May (22 days; no sample was collected on the 14 April 2019)

for approximately 90% of the total community during the period of highest recorded chlorophyll concentrations (Figures 2B and 3B). Other algae with PR2 classifications (diatoms, archaeplastids, cryptophytes, and haptophytes) collectively accounted for approximately 20% of the total community at the beginning of our sampling period, but were observed at low relative abundances by Day 13 in 2019.

Changes in the relative abundances of well-defined heterotrophic protists during 2018 and 2019 were similar despite differences in phytoplankton community composition, and generally constituted minor components of the total read count. The largest increase in MArine STramenopile lineages (MAST) and choanoflagellates, which are globally distributed bacterivorous protists, occurred after the decline of diatoms in both years. Cercozoan and syndinean taxa also exhibited higher relative abundances following the diatom decline in both years; however, increases in cercozoan relative abundances were more pronounced during 2019 (Figure 3). The cercozoan genus is diverse and contains both parasitic and non-parasitic taxa, whereas syndinean taxa are believed to be globally distributed parasitic protists. Ciliates were present throughout both sampling periods at notable relative abundances but were more abundant and diverse during 2019 (Days 18 and 19 in Figure 3B). Several unclassifiable ochrophytes were present throughout both sampling periods, whereas non-cercozoan rhizarian taxa were nearly undetectable throughout the sampling periods of both years.

Shared and unique diatom and dinoflagellate ASVs

The diversity and daily changes in relative abundances of the dominant taxa (approximately genus-level groupings) within the diatom and dinoflagellate assemblages during 2018 and 2019 blooms revealed that 6 of the 60 total classified diatoms (10%) and 5 of the 66 total classified dinoflagellates (8%) accounted for the majority of total reads in their respective assemblages. Three of six abundant diatom taxa dominated in 2018 (Figure S3). *Thalassiosira*, *Rhizosolenia*, and *Pseudo-nitzschia* (in order of decreasing total relative abundance) increased markedly to high proportions over 4 days and gradually declined with the pronounced rise and fall in chlorophyll values during the 2018 bloom (Figure 4A). Three different diatom taxa, *Guinardia*, *Chaetoceros*, and *Leptocylindrus*, accounted for the highest proportion of the diatom assemblage in 2019, although fewer total diatom reads were observed that year (Figures 4C vs. 4A, S4). The three dominant taxa during 2019 gradually declined from their highest proportions observed on Day 1 with the exception of Day 10, and all six diatom taxa were nearly undetectable by Day 13 (Figures 3B and 4C).

The five most abundant dinoflagellate taxa observed in 2018 and 2019 were also taxonomically distinct (Figure 4B,D). There were gradual increases in the relative abundances of many dinoflagellate taxa throughout the sampling periods during both years (Figures S3 and S4). *Prorocentrum* and *Gyrodinium* became the most relatively abundant dinoflagellate taxa after the decline of diatoms in 2018 (Figure 4B) and also contained the most ASVs of the dinoflagellate

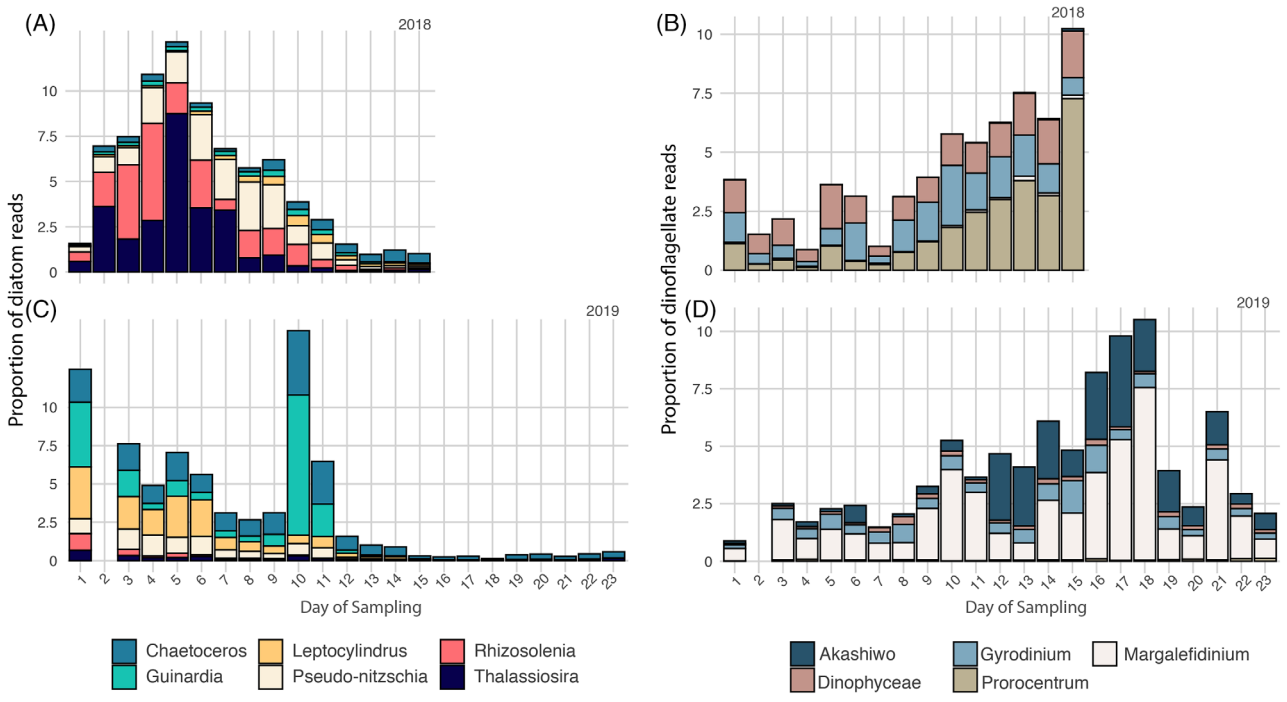

FIGURE 4 Changes in the proportion of the six diatom taxa that accounted for >10% of the diatom assemblage during 2018 (A) and 2019 (C). Changes in the proportion of the five dinoflagellate taxa that accounted for >10% of the dinoflagellate assemblage during the sampling periods in 2018 (B) and 2019 (D) where Dinophyceae represents the dinoflagellates that lacked genus-level classification in the PR2 database (v. 12). Sampling from the Santa Monica Pier (SMP) was conducted daily at 0900 from the same location and orientation on the SMP from the 16 through the 30 April 2018 (15 days), and in 2019 from the 13 April through 6 May (22 days; no sample was collected on the 14 April 2019)

assemblage in 2018. *Margalefidinium* (formerly *Cochlodinium*) and *Akashiwo* (in order of decreasing relative abundance) were the dominant dinoflagellate taxa during 2019 (Figure 4D). *Margalefidinium* was the most relatively abundant taxa when sequenced reads were summed throughout the 22-day sampling period. We identified this species as *Margalefidinium fulvescens* via light microscopy (Figure 5F,S). *Akashiwo* was relatively rare until Day 12, but subsequently increased more than 10-fold. *Margalefidinium* and *Akashiwo* reached their peak relative abundances coincident with the highest recorded chlorophyll values (~60 μg/L; Figure 4D).

The diatom taxa with the greatest relative read abundances were generally not the taxa containing the most unique ASVs (richness). For example, *Chaetoceros* was one of the least abundant taxa in 2018, but accounted for a larger fraction of ASVs than all other dominant groups with the exception of *Thalassiosira* (Figure S5A). Conversely, dinoflagellate taxa containing the greatest number of ASVs generally accounted for greatest relative abundance in both years (Figure S5C).

An examination of the number of diatom and dinoflagellate ASVs that were observed only in 2018 or 2019, versus those that were shared across both years, revealed that the majority of diatom ASVs (103) and dinoflagellate ASVs (129) were shared across both years, whereas comparatively few ASVs from both assemblages were unique to 2018 or 2019 sampling periods (Figure 6A,C). Examination of the unique ASVs that accounted for more than 1% of the total reads from the diatom or dinoflagellate assemblage in either year revealed that nearly all (>95%) of the most abundant diatom and dinoflagellate ASVs were shared across both years; 33 of the 34 diatom and 30 of the 31 dinoflagellate ASVs greater than 1% were shared in both years. The percent abundances of each varied between the 2 years (Figure 6B,D). One diatom ASV classified as *Thalassiosira* was found during 2018 but

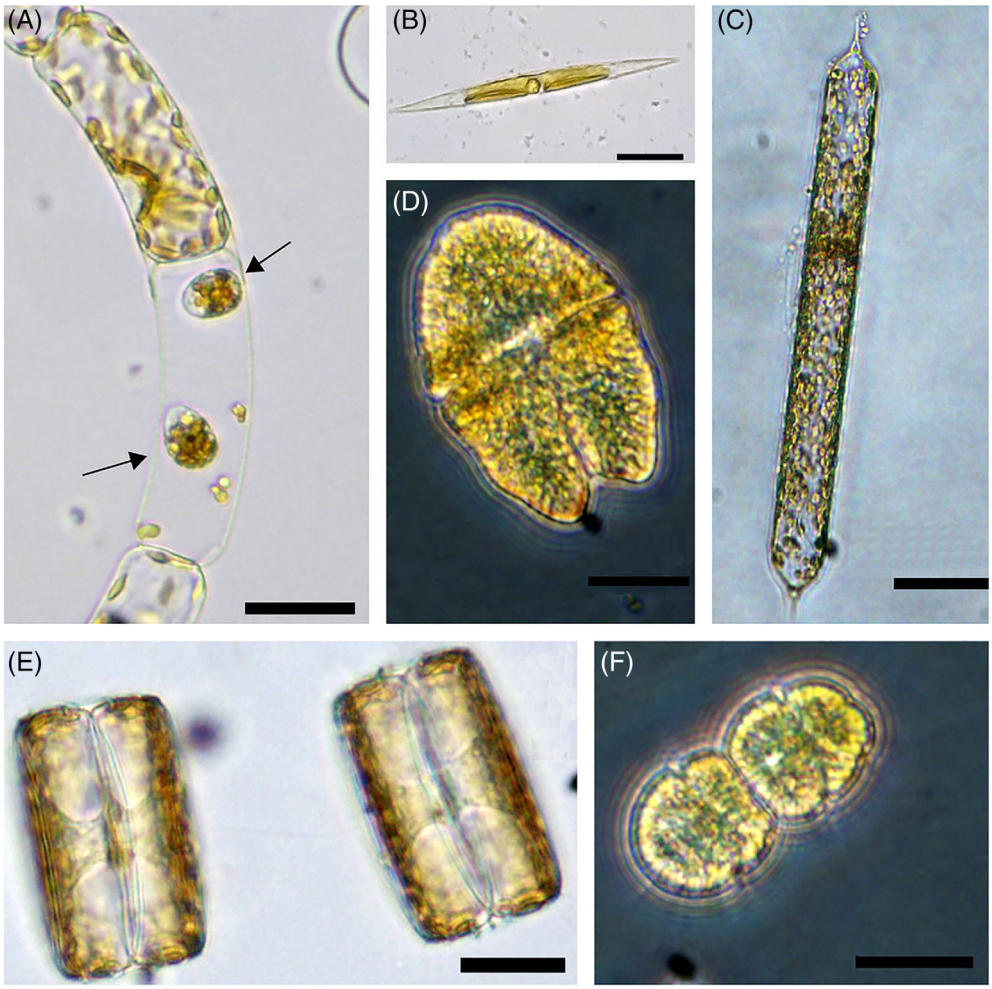

FIGURE 5 Images taken of the dominant protistan taxa from the 2018 and 2019 blooms via light microscopy. Black scale bar = 20 μm. (A) Cryothecomonas sp. (Cercozoa) infecting Guinardia sp., (B) Pseudo-nitzschia sp., (C) Rhizosolenia sp., (D) Akashiwo sp., (E) Thalassiosira eccentrica, (F) Margalefidinium fulvescens

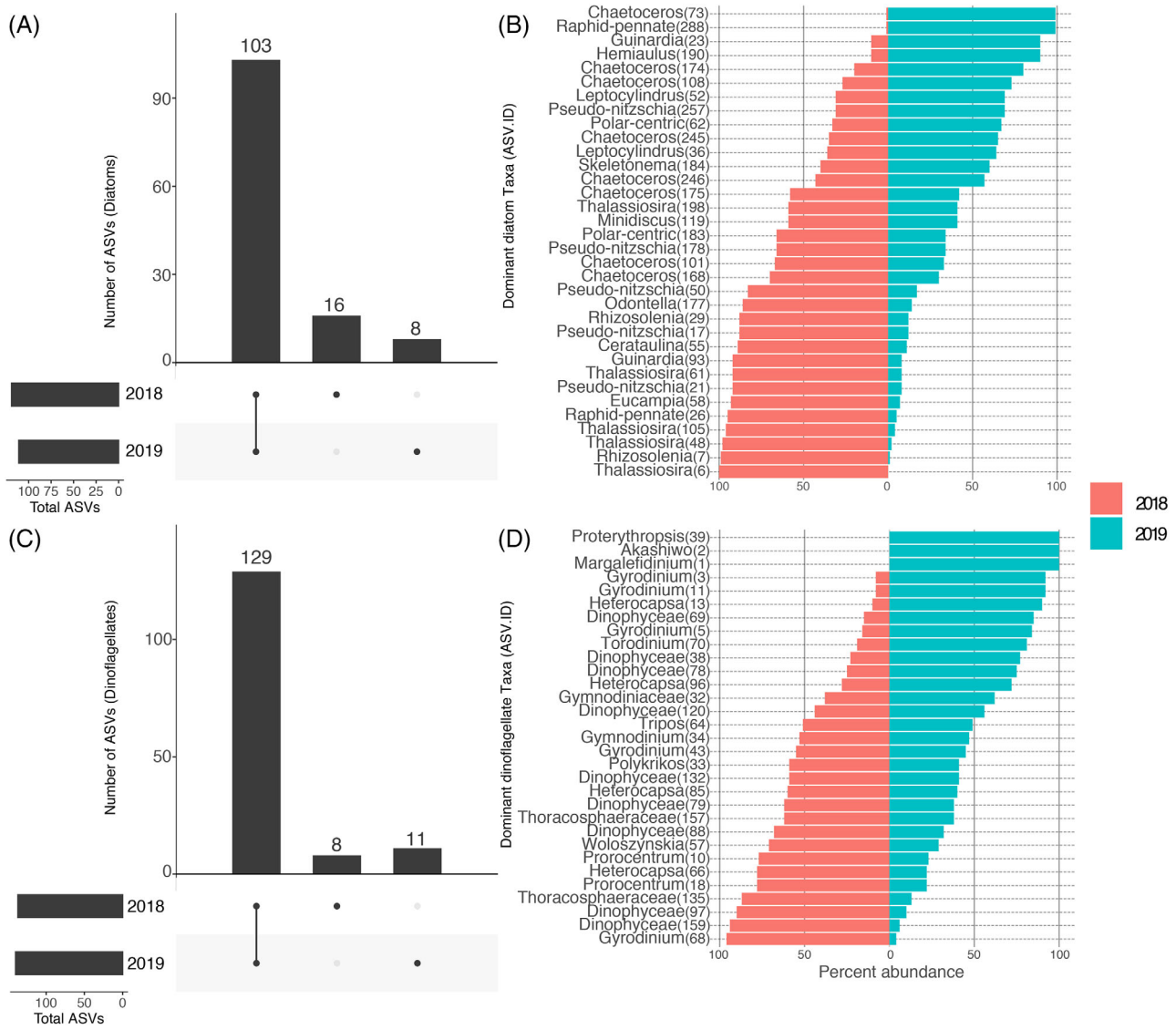

FIGURE 6 Upset plots (left column) illustrating the number of unique and shared diatom (A) and dinoflagellate (C) ASVs observed in 2018 and 2019. Vertical bars represent the number of ASVs present in both years (left), only 2018 (middle), or only 2019 (right); horizontal bars represent the total number of ASVs counted for each year. Pyramid diagrams (right column) illustrating the percent overlap and taxonomic classification of the diatom (B) or dinoflagellate (D) ASVs that accounted for at least 1% relative (read) abundance of their respective assemblages.

not 2019, and one dinoflagellate ASV classified as *Proterythropsis* was found during 2019 but not 2018.

Network analysis of ecologically significant associations

A sparse co-association network of positive and negative associations was constructed using ASVs from the 2018 and 2019 datasets to examine community-level connectivity and species interactions that may have influenced the temporal changes in community structure of the protistan assemblage (Figure 7). Structural features of both the 2018 and 2019 association networks exhibited modularity and "small-world" characteristics (Watts and Strogatz, 1998) (Table 1). The degree distribution, which provides the probability that a randomly selected node in the network has *n* number of associations, decreased asymptotically; the majority of nodes had relatively few associations; the rare exceptions – hub nodes – contained up to 91 and 115 associations in 2018 and 2019, respectively (Table 1).

Diatoms accounted for the majority of positive and negative associations in 2018 (23% and 21%, respectively) and in 2019 (20% and 18%; Figures 7, S6). The majority of the positive diatom associations found in both years occurred with other diatom nodes, and nodes corresponding to ciliates in 2019. The majority of negative diatom associations in 2018 were with

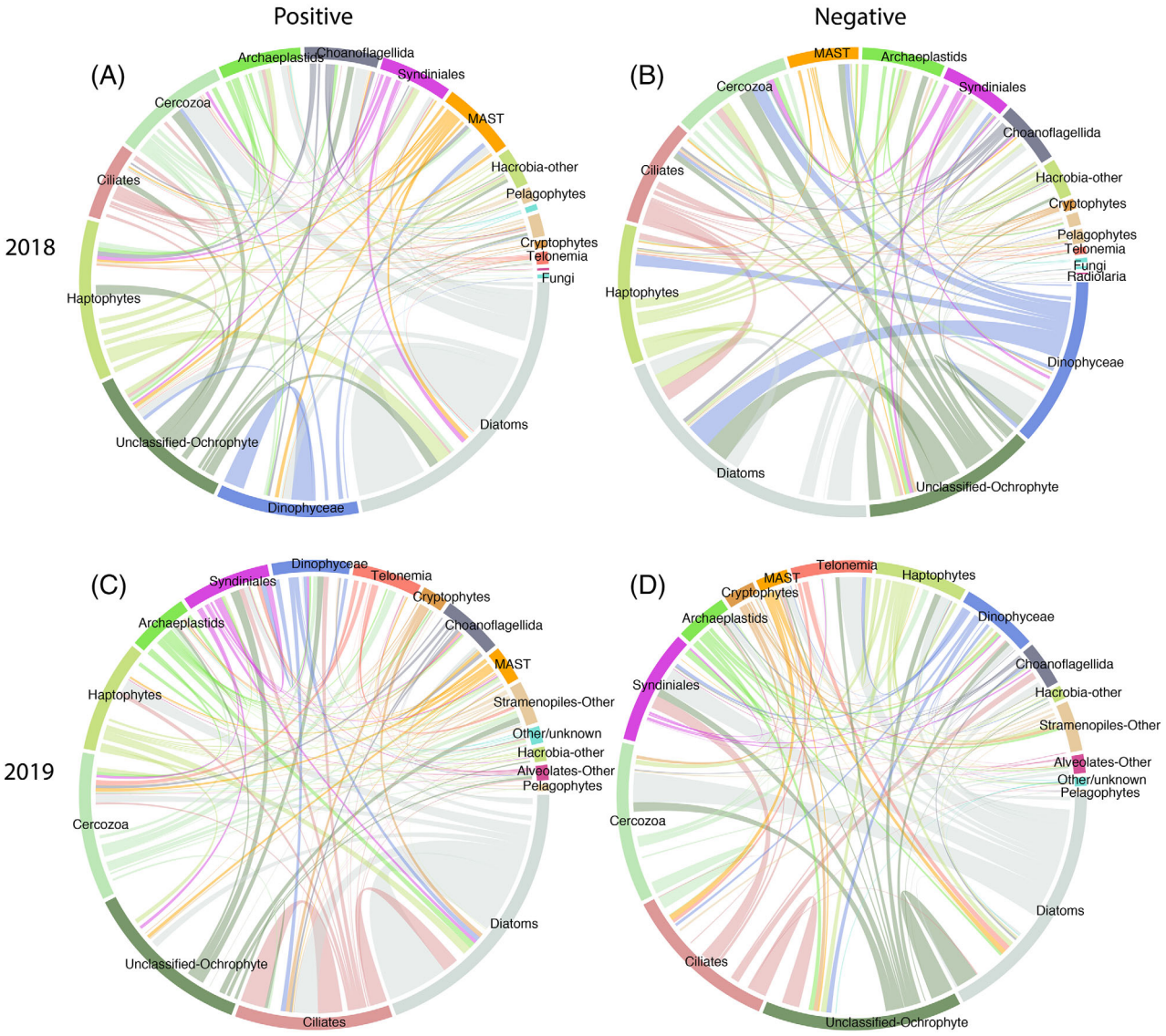

FIGURE 7 Negative (A and C) and positive (B and D) associations among major taxonomic groups during the 2018 (top) and 2019 (bottom) sampling periods. Ribbon width is proportional to the number of associations between and among species within the major taxonomic groups.

TABLE 1 Quantitative properties of networks produced using the 2018 and 2019 sample sets

Year	Nodes	Links	Avg Path	Diamet	AD	MD	MaxD	CC
2018	783	7383	4.13	0.61	19	9	90	0.45
2019	733	7993	4.09	0.55	22	10	114	0.48

Note: Nodes and links represent the number of taxa and associations in each network, respectively. Average Path length (Avg Path) represents the average number of nodes in the shortest path for all possible pairs of nodes. Network diameter (Diamet) represents the shortest distance between the two most distant nodes in the network. Degree is defined as the number of links (associations) connected to a node. AD, MD, and MaxD represent the average, median, and maximum degrees, respectively. The clustering coefficient (CC) value is a measure the modularity of a typical neighbourhood of highly connected nodes and accounts for the number of triangles in the network.

dinoflagellates (Figure 7B), whereas the majority of negative diatom associations in 2019 were with syndinean and cercozoan taxa (some possible cercozoan parasites; Figure 7D, Table S4). Associations between *Cryothecomonas* and known diatom targets (*Guinardia* sp., *Rhizosolenia* sp., and *Thalassiosira* sp.) were identified in both years (Table S4) (Drebes et al., 1996; Schnepf & Kühn, 2000; Tillmann et al., 1999). Additionally, *Prymnesium parvum*, a mixotrophic haptophyte, was associated with both *Miniduscus* (2019 only) and *Thalassiosira* – two known predatory interactions (Martin-Cereceda et al., 2003; Skovgaard &

Hansen, 2003). Dinoflagellates accounted for sixfold fewer associations than diatoms in both 2018 and 2019 (Figures 7, S6; Table S4). Associations between syndinean taxa and known dinoflagellate targets included *Prorocentrum* (2019), *Gymnodinium* (2018), and *Akashiwo* (2019) (Alves-de-Ssouza et al., 2012; Park et al., 2002); Margalefidinium (Cochlodinium) associations were only identified during 2018 despite being the numerically dominant taxa in 2019 (Table S4) (Kim & Park, 2014; Park et al., 2004).

DISCUSSION

Our study examining the abiotic and biotic controls of protistan community composition during spring blooms in two consecutive years in Santa Monica Bay revealed that diatoms dominated the community following both wind-driven upwelling events. Consistent with previous findings, diatoms in the region are highly successful in response to the general physical/chemical conditions brought about by upwelling. However, substantially different diatom taxa dominated the two blooms in our 2-year study despite somewhat similar environmental forcing factors and conditions (Figures 1 and 2; Figure S1), and despite strong overlap in the identity of the abundant ASVs in both years (Figure 6). Also significant was our finding that, while both diatom blooms declined following the depletion of inorganic nutrients (primarily nitrogen) in the days following both upwelling events, the phytoplankton assemblage during 2019, but not 2018, transitioned to a massive, long-lived dinoflagellate bloom. Minor differences in the magnitude, timing, and frequency of wind events (and consequent differences in water chemistry and physics) may explain some of the community differences between the 2 years. Our network analysis and microscopy also revealed interactions between parasites and diatoms that may have played a pivotal role in diatom bloom senescence and dinoflagellate succession during 2019.

Wind-driven upwelling shaped overall community composition, but subtleties controlled species dominance

Environmental parameters characteristic of upwelling were captured during both 2018 and 2019 (decreased temperature, increased salinity, elevated nutrient concentrations), and therefore do not immediately explain the distinct diatom communities observed during the early portion of the sampling period during each year. Elevated nutrient concentrations observed at the beginning of both sampling periods were indicative of strong upwelling events in the region (Howard et al., 2014). Marginally lower minimal temperature (12.6 vs. 13.6°C), higher maximal salinity (33.64 vs. 33.62 PSU), higher maximal nitrite + nitrate concentration (10.10 vs. 8.06 μM), and higher maximal phosphate concentration (1.16 vs. 0.80 μM) were observed in 2018 relative to 2019 (Figures 1, 2), although sampling during 2019 appears to have begun during nutrient drawdown rather than at peak nutrient concentrations (Figure 2B).

Phytoplankton bloomed to comparable magnitudes (i.e. chlorophyll concentrations of 17–18 μg/L) following upwelling events on Days 4 or 5 of sampling in both years, and both blooms were classified as major blooms for the region (Figure 2; Table S1) (Seubert et al., 2013). Both assemblages were dominated by diatoms, as predicted by general paradigm regarding their rapid response to upwelling conditions. However, community analysis of the blooms via 18S rRNA gene V4 sequencing revealed very different dominant taxonomic composition each year. Diatoms identified as *Thalassiosira*, *Rhizosolenia*, and *Pseudo-nitzschia* dominated in 2018, whereas *Chaetoceros*, *Leptocylindrus*, and *Guinardia* dominated the diatom assemblage in 2019 (Figure 4A vs. 4C).

It is unknown if minor differences in the initial upwelling conditions led to different bloom trajectories in 2018 and 2019 with respect to diatom community composition. Cell abundances catalogued by the Southern California Coastal Ocean Observing System (SCCOOS) illustrated that cell abundances of *Pseudo-nitzschia* spp. were almost fourfold higher in March 2018 – prior to sampling – than in 2019 (https://erddap.sccoos.org/erddap/tabledap/HABs-SantaMonicaPier.html). Cell abundance information for the other numerically dominant diatom taxa from this study were likely aggregated with 'Other Diatoms'. However, upwelling strength appears to have been stronger and temporally less clearly defined as a single event during the study period in 2018 relative to 2019 (Figure 1; Figure S1B vs. C). Physical forcing but also resting periods thought to be important for the spawning of coastal blooms (Smayda, 2010; Trainer et al., 2010). Strong equatorward winds in this study with short resting periods that may have facilitated the algal response were recorded three times in April of 2018 (once prior to and twice during the sampling period) while a single strong event was recorded prior to sampling during 2019 (Figure S1). Additionally, modest peaks in nutrient concentrations were observed multiple times throughout the 15-day observation period in 2018, while increases in nutrient concentrations were muted throughout the 23-day observation period in 2019 after Day 4. We speculate that periodic, minor reinforcement of upwelling conditions may have significantly prolonged dominance of diatoms in 2018 but cannot immediately explain compositional differences of the diatom assemblages observed in the 2 years.

A massive dinoflagellate bloom succeeded the diatom bloom in 2019 but not 2018

The formation of a dinoflagellate bloom after diatom bloom senescence in 2019, was striking and mirrored other observations of diatom to dinoflagellate bloom transitions (Figures 3B and 4D) (Spilling et al., 2018; Zhang et al., 2019). Chlorophyll concentrations attained extremely high values (up to >60 μg/L) during dinoflagellate dominance in 2019, albeit day-to-day variability was substantial presumably due to patchy distribution of dinoflagellates (Figure 2B). Community dynamics during 2018 contrasted with our observations during 2019, in which diatoms bloomed, but dinoflagellates were a minor component of the community (Figures 3 and 4). Chlorophyll concentrations during both years attained similar maximum values during numerical dominance of diatoms (∼17–18 μg chlorophyll/L; Figure 2).

Pre-bloom cell abundances do not immediately explain the succession to or community composition of the dinoflagellate bloom. Although dinoflagellates appeared to be more abundant in March 2019 prior to the bloom, *Margalefidinium (Cochlodinium)* was not counted and diatoms also appeared to have greater abundances compared with 2018 (https://erddap.sccoos.org/erddap/tabledap/HABs-SantaMonicaPier.html).

It is possible that differences in the physical forcing factors during each year may explain the succession of dinoflagellates following the diatom bloom during 2019 but not 2018. Multiple wind events were observed prior to, and during our study in 2018 (12, 16–17, 19–20 April), while extended quiescent wind conditions, warmer water temperatures, and a presumed stabler water column followed the single notable upwelling event just prior to our study period in 2019 (9–12 April; Figure S1C). As noted above, continued dominance of diatoms during the more turbulent 2018 study period and succession of dinoflagellates during the warmer, quiescent period of 2019 are consistent with expectations of the general conditions promoting either type of bloom (Margalef, 1978; Smayda, 2010; Smayda & Reynolds, 2001).

Additionally, while differences in community composition during the latter portions of the observational periods in 2018 and 2019 may be related to subtle differences in physical forcing between the 2 years (specifically the success of dinoflagellates in 2019 but not 2018), the magnitude of the dinoflagellate-dominated bloom is more difficult to explain. Chlorophyll concentrations observed from Day 16 through 21 in 2019 were approximately two to fourfold higher than the values observed during the peak diatom bloom (Day 4), despite the absence of significant wind forcing or nutrient increases after diatom senescence (Day 4 in Figure 2B; Figure S1C). The source of nutrients that supported such a bloom is therefore not obvious. However, mixotrophy (here, the consumption of prey by photosynthetic dinoflagellates) is a common strategy among many dinoflagellate species to acquire nutrients not readily available to purely photosynthetic taxa (Hansen, 2011; Stoecker, 1999; Stoecker et al., 2017).

Vertical migration is also a long-known behaviour among dinoflagellates in nearshore coastal communities for acquiring nutrients sequestered in deeper waters or sediments (Eppley et al., 1968; Koizumi et al., 1996). Interestingly, Park et al. (2019) documented a 15 m diel vertical migration in a red tide event near Namhae Island, Korea by *Margalefidinium* (*Cochlodinium*) *polykrikoides* (Park et al., 2019). *Margalefidinium* was a dominant taxon in the dinoflagellate bloom that appeared at the SMP in 2019 (Figures 4D and 5F). We speculate that mixotrophy and/or vertical migration coupled to the lack of physical forcing events may explain – in part – the massive bloom of dinoflagellates observed during 2019.

Parasitic protists may have contributed to diatom bloom senescence and community succession

Changes in the relative abundances of diatoms and putative parasites captured with 18S rRNA (cDNA) sequencing, in conjunction with associations catalogued via network analysis and microscopy, indicate that parasites may have played a significant role during the diatom blooms in both years, but a particularly important role in bringing about diatom bloom senescence during 2019. Cercozoan and syndinean ASVs exhibited increases in relative abundance coincident with the decline of the diatom bloom in 2019, in which the cercozoan increase was particularly noteworthy (Figure 3B). Network analysis during 2019 revealed strong associations between both cercozoan and syndinean taxa with diatoms (Figure 7C,D, Table S4). Cercozoan associations with diatoms outnumbered syndinean associations with diatoms; however, both taxa exhibited more negative associations with diatoms than positive (Table S4).

Interactions between diatoms and parasitic cercozoan species such as *Cryothecomonas* spp. have been previously observed, and strong associations identified between *Cryothecomonas* spp. and multiple known diatom targets – including *Guinardia*, *Thalassiosira*, and *Rhizosolenia* – during this study support the conclusion that parasites may have influenced diatom bloom dynamics in both 2018 and 2019 (Table S4) (Drebes et al., 1996; Peacock et al., 2014; Schnepf & Kühn, 2000; Scholz et al., 2016; Tillmann et al., 1999). Intriguingly, the number of syndinean associations with diatom taxa in this study either greatly exceeded the number of syndinean associations with dinoflagellates

(2019; 234 diatom vs. 83 dinoflagellate) or were numerically comparable (2018; 127 diatom vs. 123 dinoflagellate) – a finding that contrasts the scarcity of known interactions between syndinean and diatom taxa (Markussen Bjorbækmo et al., 2019). This contrast may underscore the strength of network analysis for studying the ecology of free-living parasites and the need for further classification of laboratory-confirmed interactions.

Similar temporal dynamics and cercozoan associations with diatoms were observed during a spring bloom in the San Pedro Channel, California (Berdjeb et al., 2018). Conversely, in 2018, we observed slight increases in cercozoan and syndinean ASVs during the decline of the diatom bloom, but the majority of the associations captured between both cercozoan and syndinean groups with diatoms during that year were positive (Figure 7, Table S4).

Parasite associations have been characterized as both positive and negative in ecological association networks. Positive associations have been thought to represent cases where the parasites did not produce enough mortality to produce a negative relationship (Berdjeb et al., 2018; Faust & Raes, 2012; Fuhrman et al., 2015). We speculate that the mortality caused by parasites in our 2019 study may have been sufficient to yield the observed negative associations between cercozoan and syndinean parasites with diatoms.

Cryothecomonas sp., a known cercozoan parasite, was identified feeding on *Guinardia* spp., one of the numerically dominant diatom genera in 2019, via light microscopy (Figure 5A). *Cryothecomonas* contains many specialist and generalist species that are capable of forming infective and virulent propagules (zoospores) with specialized structures for penetrating the frustules of diatom hosts (Drebes et al., 1996). Species of *Cryothecomonas* have been found in plankton samples at temperatures ranging from 14 to 17°C, consistent with the present study (Drebes et al., 1996; Markussen Bjorbækmo et al., 2019; Peacock et al., 2014; Schnepf & Kühn, 2000; Scholz et al., 2016; Tillmann et al., 1999). No parasites were observed by microscopy during 2018, but the dynamics of cercozoan and syndinean taxa during the decline of the diatom bloom during that year, and their generally positive associations with diatoms, appears to indicate a low level of infection during 2018 compared to 2019.

Parasitic infection and lysis have biogeochemical implications due to the physical nature and chemical properties of material released by parasitized cells. It is probable that lysis debris not consumed by parasites contains labile dissolved organic matter, as well as the host's empty silica frustule. Parasitism may therefore be more analogous to DOM and POM release resulting from lytic infection by marine viruses (Fuhrman, 1999), rather than feeding by micro- or meso-zooplankton. Free-living parasites and zoospores are also smaller than their hosts and thereby vulnerable to predation by a diverse range of phagotrophic protists significantly smaller than the host (Massana et al., 2009; Piwosz et al., 2021; Scholz et al., 2016; Sherr & Sherr, 2002). Such overall reduction in particle size may reduce the amount of carbon and energy transferred up plankton food chains.

Dissolved nutrients released from infected cells may have contributed to the success of dinoflagellates after diatom senescence in 2019. The possible utilization of the DON and DOP released from infected hosts by dinoflagellate taxa is consistent with recent studies that have illustrated the utilization of a wide variety of dissolved organic nitrogen and phosphorus distinct from diatoms, (Alexander et al., 2015). Targeted metatranscriptomic assays during such regime changes may shed light on the adaptive strategies of dinoflagellates by identifying the differentially expressed genes related to nutrient uptake and metabolism (Hu, Liu, et al., 2018). Indeed, a recent study investigating gene expression during the shift from a diatom-dominated bloom to dinoflagellate dominance revealed differences in nutrient uptake, energy acquisition, and catabolic strategies between the dominant diatom taxa and the dominant dinoflagellate, *Prorocentrum donghaiense* (Zhang et al., 2019).

Zoosporic parasites are diverse and may have several impacts in plankton communities (Guillou et al., 2008; Scholz et al., 2016). They may increase diversity in food webs (Dunne et al., 2013), dominate food web links in ecological networks (Lafferty et al., 2006; Lima-Mendez et al., 2015), they are globally distributed throughout the water column (de Vargas et al., 2015; Ollison et al., 2021), and can have a demonstrable impact on species succession during algal blooms (Chambouvet et al., 2008). Although the magnitude of their impact is unclear, network analysis and direct observations together show that parasites likely played an ecological role in diatom bloom dynamics during both 2018 and 2019 and should be considered in future modelling efforts of upwelling bloom dynamics.

Heterotrophy by tiny predators (MAST) was elevated during bloom senescence

We observed an increase in the relative abundance of MAST lineages coincident with the decline of both diatom blooms, and substantial direct associations between MAST and diatoms during both 2018 and 2019. Comparable amounts of negative and positive associations were captured in 2018, whereas only negative associations were captured in 2019.

Results from environmental surveys have indicated that many heterotrophic nano-flagellates, which are the most important consumers and remineralizers of

heterotrophic bacteria and picophytoplankton in marine ecosystems, are novel MAST lineages (Lin et al., 2012; Massana et al., 2006; Massana et al., 2009). Several of the 12 known lineages have been found throughout the global ocean, but the specific trophic roles of each is unknown. For example, MAST-3 is thought to contain parasitic lineages based on sequence similarity to *Solenicola setigera*, a known diatom parasite (Gómez, 2007; Gómez et al., 2011). Moreover, heterotrophic bacteria as consumers of labile DOM and POM are known to mobilize and proliferate during algal blooms in decline (Buchan et al., 2014; Needham & Fuhrman, 2016; Teeling et al., 2012). The increase in the relative abundance of MAST during the demise of diatom blooms in 2018 and 2019 was likely linked to possible increases in prey availability (the mobilization of bacterial prey and/or the release of free-living zoosporic parasites; Figure 3). However, the possibility of MAST lineages acting as diatom parasites during either year cannot be excluded.

Protistan community structure and the core community of Santa Monica Bay

Molecular methods for studying protistan diversity and community composition throughout the global ocean have resulted in estimates of community richness that have greatly surpassed earlier estimates based on traditional methods (i.e. microscopy) of species identification and quantification (Caron et al., 2012; de Vargas et al., 2015; Pedros-Alio et al., 2018). Recent genetic studies have shown that the vast pool of (mostly rare) protistan species enables communities to vary greatly over large and fine spatiotemporal gradients (Balzano et al., 2015; Caron & Countway, 2009; de Vargas et al., 2015; Hu et al., 2016; Ollison et al., 2021).

In this study, thousands of unique ASVs were catalogued in Santa Monica Bay during the spring upwelling season in two different years (Figure S2B; Table S2). However, the same diatom (33) and dinoflagellate (30) ASVs each consistently accounted for at least 1% or more of the community across both years (Figure 6B,D). The repeated appearance of the most abundant ASVs, which likely represent subspecies-level diversity (Caron & Hu, 2018), despite the vast amounts of species richness and spatiotemporal fluctuation associated with the annual cycle in the California Current (Hickey, 1979) is consistent with a *core community* of diatom and dinoflagellate taxa in Santa Monica Bay that constitute a seed bank for blooms during spring upwelling (Table S3). The core ASVs fell within relatively few unique taxonomic groupings at approximately genus level, many of which have been previously identified from water samples collected along the Southern California coast, including well-known HAB taxa (Barth et al., 2020; Kim et al., 2009; Shipe et al., 2008; Venrick, 2012). It is not yet clear how the aforementioned abiotic and biotic forces work in concert with other physical and chemical factors not characterized in this study to select the dominant, blooming taxa from this core during a particular spring bloom season, or what anticipated climate-induced changes (wind, temperature, and chemical properties) portend for bloom composition, magnitude, duration, and phenology (Capone & Hutchins, 2013; Fu et al., 2012; Griffith et al., 2019; Howes et al., 2015; Hutchins et al., 2019; Hutchins & Boyd, 2016; Hutchins & Fu, 2017; Tatters et al., 2018; Vikebø et al., 2019; Weatherdon et al., 2016). We hypothesize that the ecological redundancy represented by the taxonomic identities of the core community indicates an adaptable community that may be able to maintain biogeochemical processes in spite of small or dramatic changes in environmental factors (Caron & Countway, 2009).

This work extends the findings of DNA-based high-frequency sampling metabarcoding studies of phytoplankton blooms by sequencing 18S rRNA gene transcripts (RNA) daily throughout two blooms in the Southern California Coastal upwelling regime. This approach enabled us to examine metabolically active taxa and contrast changes in relative abundances that are not distorted by genomic variation in 18S rRNA gene copies or chloroplasts per cell. In this study as well as other metabarcoding-based studies, diatoms bloomed to numerical dominance immediately following upwelling; smaller flagellated taxa were in greater relative abundance following diatom senescence; taxa within both guilds exhibited intra-guild successions on short time scales (Needham et al., 2018; Needham & Fuhrman, 2016; Trefault et al., 2021). Accordingly, and consistent with other findings, we have shown that microbial communities can exhibit rapid community turnover with multiple taxa exhibiting many differential responses within the community (Wilson et al., 2021). The traditional view of the impact of nutrients and even small differences in physical-forcing was augmented in this study; however, similar to other studies, we have illustrated that species interactions are likely an important driver of community succession (Berdjeb et al., 2018; Fuhrman et al., 2015; Needham & Fuhrman, 2016; Trombetta et al., 2020).

ACKNOWLEDGEMENTS

The authors are grateful to the staff of the Heal the Bay Aquarium for their gracious logistical support and space for sample processing at the pier: Apryl Boyle, Jenna Segal, Marslaidh Ryan, and staff. The authors are also grateful to Jed Fuhrman and his lab for support with sampling and transportation. A very special thanks to Markie Hu for assistance with the sampling effort. Thanks to Jake Weisman and Jacob Cram for insightful conversations regarding the network analysis strategies used in this work and comments on this

manuscript, and to Patrick Schloss and Samantha Gleich for assistance with data handling and critique regarding visualization. This work was supported by the National Science Foundation #1136818 (David A. Caron).

CONFLICT OF INTEREST

The author declares that there is no conflict of interest that could be perceived as prejudicing the impartiality of the research reported.

DATA AVAILABILITY STATEMENT

Raw 18S sequence data is available through NCBI under accession number PRJNA480318.

ORCID

Gerid A. Ollison https://orcid.org/0000-0002-0032-5601
Sarah K. Hu https://orcid.org/0000-0002-4439-1360

REFERENCES

Alexander, H., Rouco, M., Haley, S.T., Wilson, S.T., Karl, D.M. & Dyhrman, S.T. (2015) Functional group-specific traits drive phytoplankton dynamics in the oligotrophic ocean. *Proceedings of the National Academy of Sciences of the United States of America*, 112, E5972–E5979.

Alves-de-Ssouza, C., Varela, D., Iriarte, J.L., González, H.E. & Guillou, L. (2012) Infection dynamics of Amoebophryidae parasitoids on harmful dinoflagellates in a southern Chilean fjord dominated by diatoms. *Aquatic Microbial Ecology*, 66, 183–197.

Auinger, B.M., Pfandl, K. & Boenigk, J. (2008) Improved methodology for identification of Protists and microalgae from plankton samples preserved in Lugol's iodine solution: combining microscopic analysis with single-cell PCR. *Applied and Environmental Microbiology*, 74, 2505–2510.

Azam, F., Fenchel, T., Field, J.G., Gray, J.S., Meyer-Reil, L.A. & Thingstad, F. (1983) The ecological role of water-column microbes in the sea. *Marine Ecology Progress Series*, 10, 257–263.

Balzano, S., Abs, E. & Leterme, S.C. (2015) Protist diversity along a salinity gradient in a coastal lagoon. *Aquatic Microbial Ecology*, 74, 263–277.

Barth, A., Walter, R.K., Robbins, I. & Pasulka, A. (2020) Seasonal and interannual variability of phytoplankton abundance and community composition on the central coast of California. *Marine Ecology Progress Series*, 637, 29–43.

Berdjeb, L., Parada, A., Needham, D.M. & Fuhrman, J.A. (2018) Short-term dynamics and interactions of marine protist communities during the spring-summer transition. *The ISME Journal*, 12, 1907–1917.

Bolyen, E., Rideout, J.R., Dillon, M.R., Bokulich, N.A., Abnet, C.C., Al-Ghalith, G.A. et al. (2019) Reproducible, interactive, scalable and extensible microbiome data science using QIIME 2. *Nature Biotechnology*, 37, 852–857.

Buchan, A., LeCleir, G.R., Gulvik, C.A. & Gonzalez, J.M. (2014) Master recyclers: features and functions of bacteria associated with phytoplankton blooms. *Nature Reviews. Microbiology*, 12, 686–698.

Buesseler, K.O. (1998) The decoupling of production and particulate export in the surface ocean. *Global Biogeochemical Cycles*, 12, 297–310.

Capone, D.G. & Hutchins, D.A. (2013) Microbial biogeochemistry of coastal upwelling regimes in a changing ocean. *Nature Geoscience*, 6, 711–717.

Caron, D.A. & Countway, P.D. (2009) Hypotheses on the role of the protistan rare biosphere in a changing world. *Aquatic Microbial Ecology*, 57, 227–238.

Caron, D.A., Countway, P.D., Jones, A.C., Kim, D.Y. & Schnetzer, A. (2012) Marine protistan diversity. *Annual Review of Marine Science*, 4, 467–493.

Caron, D.A. & Hu, S.K. (2018) Are we overestimating Protistan diversity in nature? *Trends in Microbiology*, 27, 197–205.

Chambouvet, A., Morin, P., Marie, D. & Guillou, L. (2008) Control of toxic marine dinoflagellate blooms by serial parasitic killers. *Science*, 322, 1254–1257.

Charvet, S., Vincent, W.F. & Lovejoy, C. (2014) Effects of light and prey availability on Arctic freshwater protist communities examined by high-throughput DNA and RNA sequencing. *FEMS Microbiology Ecology*, 88, 550–564.

Chavez, F.P. & Messié, M. (2009) A comparison of eastern boundary upwelling ecosystems. *Progress in Oceanography*, 83, 80–96.

Checkley, D.M. & Barth, J.A. (2009) Patterns and processes in the California current system. *Progress in Oceanography*, 83, 49–64.

Conway, J.R., Lex, A., & Gehlenborg, N. (2017) UpSetR: an R package for the visualization of intersecting sets and their properties. Bioinformatics, 33, 2938-2940.

Csardi, G. & Nepusz, T. (2005) The igraph software package for complex network research. *InterJournal Complex Systems*, 1695.

Davis, N.M., Proctor, D.M., Holmes, S.P., Relman, D.A., & Callahan, B.J. (2018) Simple statistical identification and removal of contaminant sequences in marker-gene and metagenomics data. *Microbiome*, 6, 226.

de Vargas, C., Audic, S., Henry, N., Decelle, J., Mahe, F., Logares, R. et al. (2015) Eukaryotic plankton diversity in the sunlit ocean. *Science*, 348, 1261605–1261601.

Drebes, G., Kühn, S.F., Gmelch, A. & Schnepf, E. (1996) *Cryothecomonas aestivalis sp*. nov., a colourless nanoflagellate feeding on the marine centric diatom *Guinardia delicatula* (Cleve) Hasle. *Helgoland Wiss Meeresunters*, 50, 497–515.

Dunne, J.A., Lafferty, K.D., Dobson, A.P., Hechinger, R.F., Kuris, A. M., Martinez, N.D. et al. (2013) Parasites affect food web structure primarily through increased diversity and complexity. *PLoS Biology*, 11, e1001579.

Eppley, R.W., Holm-Hansen, O. & Strickland, J.D.H. (1968) Some observations on the vertical migration of dinoflagellates. *Journal of Phycology*, 4, 333–340.

Falkowski, P.G., Barber, R.T. & Victor Smetacek, V. (1998) Biogeochemical controls and feedbacks on ocean primary production. *Science*, 281, 200–206.

Faust, K., Lima-Mendez, G., Lerat, J.S., Sathirapongsasuti, J.F., Knight, R., Huttenhower, C. et al. (2015) Cross-biome comparison of microbial association networks. *Frontiers in Microbiology*, 6, 1200.

Faust, K. & Raes, J. (2012) Microbial interactions: from networks to models. *Nature Reviews. Microbiology*, 10, 538–550.

Field, C.B., Behrenfeld, M.J., James, T., Randerson, J.T. & Falkowski, P.G. (1998) Primary production of the biosphere: integrating terrestrial and oceanic components. *Science*, 281, 237–240.

Friedman, J., Hastie, T. & Tibshirani, R. (2007) Sparse inverse covariance estimation with the graphical lasso. *Biostatistics*, 9, 432–441.

Fu, F.X., Tatters, A.O. & Hutchins, D.A. (2012) Global change and the future of harmful algal blooms in the ocean. *Marine Ecology Progress Series*, 470, 207–233.

Fuhrman, J.A. (1999) Marine viruses and their biogeochemical and ecological effects. *Nature*, 399, 541–548.

Fuhrman, J.A., Cram, J.A. & Needham, D.M. (2015) Marine microbial community dynamics and their ecological interpretation. *Nature Reviews. Microbiology*, 13, 133–146.

Gómez, F. (2007) The consortium of the protozoan *Solenicola setigera* and the diatom *Leptocylindurs mediterraneus* in the Pacific Ocean. *Acta Protozoologica*, 46, 15–24.

Gómez, F., Moreira, D., Benzerara, K. & López-García, P. (2011) *Solenicola setigera* is the first characterized member of the abundant and cosmopolitan uncultured marine stramenopile group MAST-3. *Environmental Microbiology*, 13, 193–202.

Gong, W. & Marchetti, A. (2019) Estimation of 18S gene copy number in marine eukaryotic plankton using a next-generation sequencing approach. *Frontiers in Marine Science*, 6, 219.

Griffith, A.W., Doherty, O.M. & Gobler, C.J. (2019) Ocean warming along temperate western boundaries of the Northern Hemisphere promotes an expansion of *Cochlodinium polykrikoides* blooms. *Proceedings of the Royal Society B: Biological Sciences*, 286, 20190340.

Guillou, L., Viprey, M., Chambouvet, A., Welsh, R.M., Kirkham, A.R., Massana, R. et al. (2008) Widespread occurrence and genetic diversity of marine parasitoids belonging to Syndiniales (Alveolata). *Environmental Microbiology*, 10, 3349–3365.

Gutierrez-Rodriguez, A., Stukel, M.R., Lopes Dos Santos, A., Biard, T., Scharek, R., Vaulot, D. et al. (2018) High contribution of Rhizaria (Radiolaria) to vertical export in the California current ecosystem revealed by DNA metabarcoding. *The ISME Journal*, 13, 964–976.

Hansen, P.J. (2011) The role of photosynthesis and food uptake for the growth of marine Mixotrophic Dinoflagellates1. *Journal of Eukaryotic Microbiology*, 58, 203–214.

Hickey, B.M. (1979) The California current system—hypotheses and facts. *Progress in Oceanography*, 8, 191–279.

Hickey, B.M. (1992) Circulation over the Santa Monica-San Pedro Basin and shelf. *Progress in Oceanography*, 30, 37–115.

Howard, M.D.A., Sutula, M., Caron, D.A., Chao, Y., Farrara, J.D., Frenzel, H. et al. (2014) Anthropogenic nutrient sources rival natural sources on small scales in the coastal waters of the Southern California Bight. *Limnology and Oceanography*, 59, 285–297.

Howes, E.L., Joos, F., Eakin, C.M. & Gattuso, J.-P. (2015) An updated synthesis of the observed and projected impacts of climate change on the chemical, physical and biological processes in the oceans. *Frontiers in Marine Science*, 2, 56.

Hu, S.K., Campbell, V., Connell, P.E., Gellene, A.G., Liu, Z., Terrado, R. et al. (2016) Protistan diversity and activity inferred from RNA and DNA at a coastal ocean site in the eastern North Pacific. *FEMS Microbiology Ecology*, 92, fiw050.

Hu, S.K., Connell, P.E., Mesrop, L.Y. & Caron, D.A. (2018) A Hard Day's Night: diel shifts in microbial eukaryotic activity in the North Pacific subtropical gyre. *Frontiers in Marine Science*, 5, 351.

Hu, S.K., Liu, Z., Alexander, H., Campbell, V., Connell, P.E., Dyhrman, S.T. et al. (2018) Shifting metabolic priorities among key protistan taxa within and below the euphotic zone. *Environmental Microbiology*, 20, 2865–2879.

Hutchins, D.A. & Boyd, P.W. (2016) Marine phytoplankton and the changing ocean iron cycle. *Nature Climate Change*, 6, 1072–1079.

Hutchins, D.A. & Fu, F. (2017) Microorganisms and ocean global change. *Nature Microbiology*, 2, 17058.

Hutchins, D.A., Jansson, J.K., Remais, J.V., Rich, V.I., Singh, B.K. & Trivedi, P. (2019) Climate change microbiology - problems and perspectives. *Nature Reviews. Microbiology*, 17, 391–396.

Jones, A.C., Hambright, K.D. & Caron, D.A. (2018) Ecological patterns among bacteria and microbial eukaryotes derived from network analyses in a low-salinity lake. *Microbial Ecology*, 75, 917–929.

Kim, H.-J., Miller, A.J., McGowan, J. & Carter, M.L. (2009) Coastal phytoplankton blooms in the Southern California bight. *Progress in Oceanography*, 82, 137–147.

Kim, S., Jeon, C.B. & Park, M.G. (2017) Morphological observations and phylogenetic position of the parasitoid nanoflagellate *Pseudopirsonia sp*. (Cercozoa) infecting the marine diatom *Coscinodiscus wailesii* (Bacillariophyta). *Algae*, 32, 181–187.

Kim, S. & Park, M.G. (2014) *Amoebophrya* spp. from the bloom-forming dinoflagellate *Cochlodinium polykrikoides*: parasites not nested in the "Amoebophrya ceratii complex". *Journal of Eukaryotic Microbiology*, 61, 173–181.

Koizumi, Y., Uchida, T. & Honjo, T. (1996) Diurnal vertical migration of *Gymnodinium mikimotoi* during a red tide in Hoketsu Bay, Japan. *Journal of Plankton Research*, 18, 289–294.

Kranzler, C.F., Krause, J.W., Brzezinski, M.A., Edwards, B.R., Biggs, W.P., Maniscalco, M. et al. (2019) Silicon limitation facilitates virus infection and mortality of marine diatoms. *Nature Microbiology*, 4, 1790–1797.

Kudela, R.M., Pitcher, G.C., Probyn, T., Figueiras, F., Moita, T. & Trainer, V.L. (2005) Harmful algal blooms in coastal upwelling systems. *Oceanography*, 18, 184–197.

Kudela, R.M., Seeyave, S. & Cochlan, W.P. (2010) The role of nutrients in regulation and promotion of harmful algal blooms in upwelling systems. *Progress in Oceanography*, 85, 122–135.

Kurtz, Z.D., Muller, C.L., Miraldi, E.R., Littman, D.R., Blaser, M.J. & Bonneau, R.A. (2015) Sparse and compositionally robust inference of microbial ecological networks. *PLoS Computational Biology*, 11, e1004226.

Lafferty, K.D., Dobson, A.P. & Kuris, A.M. (2006) Parasites dominate food web links. *Proceedings of the National Academy of Sciences of the United States of America*, 103, 11211–11216.

Layeghifard, M., Hwang, D.M. & Guttman, D.S. (2017) Disentangling interactions in the microbiome: a network perspective. *Trends in Microbiology*, 25, 217–228.

Lima-Mendez, G., Faust, K., Henry, N., Decelle, J., Colin, S., Carcillo, F. et al. (2015) Determinants of community structure in the global plankton interactome. *Science*, 348, 6237.

Lin, Y.C., Campbell, T., Chung, C.C., Gong, G.C., Chiang, K.P. & Worden, A.Z. (2012) Distribution patterns and phylogeny of marine stramenopiles in the north pacific ocean. *Applied and Environmental Microbiology*, 78, 3387–3399.

Margalef, R. (1978) Life-forms of phytoplankton as survival alternatives in an unstable environment. *Oceanologica Acta*, 1, 493–509.

Markussen Bjorbækmo, M.F., Evenstad, A., Lieblein Røsæg, L., Krabberød, A.K. & Logares, R. (2019) The planktonic protist interactome: where do we stand after a century of research? *ISME*, 14, 544–559.

Martin-Cereceda, M., Novarino, G. & Young, J.R. (2003) Grazing by *Prymnesium parvum* on small planktonic diatoms. *Aquatic Microbial Ecology*, 33, 191–199.

Massana, R., Gobet, A., Audic, S., Bass, D., Bittner, L., Boutte, C. et al. (2015) Marine protist diversity in European coastal waters and sediments as revealed by high-throughput sequencing. *Environmental Microbiology*, 17, 4035–4049.

Massana, R., Terrado, R., Forn, I., Lovejoy, C. & Pedros-Alio, C. (2006) Distribution and abundance of uncultured heterotrophic flagellates in the world oceans. *Environmental Microbiology*, 8, 1515–1522.

Massana, R., Unrein, F., Rodriguez-Martinez, R., Forn, I., Lefort, T., Pinhassi, J. et al. (2009) Grazing rates and functional diversity of uncultured heterotrophic flagellates. *The ISME Journal*, 3, 588–596.

Muller, E.E.L., Faust, K., Widder, S., Herold, M., Martínez Arbas, S. & Wilmes, P. (2018) Using metabolic networks to resolve ecological properties of microbiomes. *Current Opinion in Systems Biology*, 8, 73–80.

Needham, D.M., Fichot, E.B., Wang, E., Berdjeb, L., Cram, J.A., Fichot, C.G. et al. (2018) Dynamics and interactions of highly resolved marine plankton via automated high-frequency sampling. *The ISME Journal*, 12, 2417–2432.

Needham, D.M. & Fuhrman, J.A. (2016) Pronounced daily succession of phytoplankton, archaea and bacteria following a spring bloom. *Nature Microbiology*, 1, 16005.

Needham, D.M., Sachdeva, R. & Fuhrman, J.A. (2017) Ecological dynamics and co-occurrence among marine phytoplankton, bacteria and myoviruses shows microdiversity matters. *The ISME Journal*, 11, 1614–1629.

Newman, M.E.J. (2004) Detecting community structure in networks. *The European Physical Journal B - Condensed Matter*, 38, 321–330.

Ollison, G.A., Hu, S.K., Mesrop, L.Y., DeLong, E.F. & Caron, D.A. (2021) Come rain or shine: depth not season shapes the active protistan community at station ALOHA in the North Pacific subtropical gyre. *Deep Sea Research Part I: Oceanographic Research Papers*, 170, 103494.

Park, J.G., Jeong, M.K., Lee, J.A., Cho, K.-J. & Kwon, O.S. (2019) Diurnal vertical migration of a harmful dinoflagellate, *Cochlodinium polykrikoides* (Dinophyceae), during a red tide in coastal waters of Namhae Island, Korea. *Phycologia*, 40, 292–297.

Park, M.G., Yih, W. & Coats, W.D. (2004) Parasites and phytoplankton, with special emphasis on dinoflagellate infections. *Journal of Eukaryotic Microbiology*, 51, 145–155.

Park, M.G., Cooney, S.K., Yih, W. & Coats, D.W. (2002) Effects of two strains of the parasitic dinoflagellate *Amoebophrya* on growth, photosynthesis, light absorption, and quantum yield of bloom-forming dinoflagellates. *Marine Ecology*, 227, 281–292.

Peacock, E.E., Olson, R.J. & Sosik, H.M. (2014) Parasitic infection of the diatom *Guinardia delicatula*, a recurrent and ecologically important phenomenon on the New England shelf. *Marine Ecology Progress Series*, 503, 1–10.

Pedros-Alio, C., Acinas, S.G., Logares, R. & Massana, R. (2018) Marine microbial diversity as seen by high-throughput sequencing. In: Gasol, J.M. & Kirchman, D.L. (Eds.) *Microbial ecology of the oceans*. Hoboken, NJ: John Wiley & Sons, Inc.

Piwosz, K., Mukherjee, I., Salcher, M.M., Grujčić, V. & Šimek, K. (2021) CARD-FISH in the sequencing era: opening a new universe of Protistan ecology. *Frontiers in Microbiology*, 1, 640066.

Pomeroy, L.R. (1974) The Ocean's food web, a changing paradigm. *Bioscience*, 24, 499–504.

Poulin, R. (2010) Network analysis shining light on parasite ecology and diversity. *Trends in Parasitology*, 26, 492–498.

Proulx, S.R., Promislow, D.E. & Phillips, P.C. (2005) Network thinking in ecology and evolution. *Trends in Ecology & Evolution*, 20, 345–353.

Robinson, M.D., McCarthy, D.J. & Smyth, G.K. (2010) edgeR: a bioconductor package for differential expression analysis of digital gene expression data. *Bioinformatics*, 26, 139–140.

Rottjers, L. & Faust, K. (2018) From hairballs to hypotheses-biological insights from microbial networks. *FEMS Microbiology Reviews*, 42, 761–780.

Ryther, J.H. (1969) Photosynthesis and Fish production in the sea. *Science*, 166, 72–76.

Schnepf, E. & Kühn, S.F. (2000) Food uptake and fine structure of *Cryothecomonas longipes* sp. nov., a marine nanoflagellate incertae sedis feeding phagotrophically on large diatoms. *Helgoland Marine Research*, 54, 18–32.

Scholz, B., Guillou, L., Marano, A.V., Neuhauser, S., Sullivan, B.K., Karsten, U. et al. (2016) Zoosporic parasites infecting marine diatoms - a black box that needs to be opened. *Fungal Ecology*, 19, 59–76.

Seubert, E.L., Gellene, A.G., Howard, M.D., Connell, P., Ragan, M., Jones, B.H. et al. (2013) Seasonal and annual dynamics of harmful algae and algal toxins revealed through weekly monitoring at two coastal ocean sites off southern California, USA. *Environmental Science and Pollution Research International*, 20, 6878–6895.

Sherr, E.B. & Sherr, B.F. (2002) Significance of predation by protists in aquatic microbial food webs. *Antonie Van Leeuwenhoek*, 81, 293–308.

Shipe, R.F., Leinweber, A. & Gruber, N. (2008) Abiotic controls of potentially harmful algal blooms in Santa Monica Bay, California. *Continental Shelf Research*, 28, 2584–2593.

Skovgaard, A. & Hansen, P.J. (2003) Food uptake in the harmful alga *Prymnesium parvum* mediated by excreted toxins. *Limnology and Oceanography*, 48, 1161–1166.

Smayda, T.J. (2010) Adaptations and selection of harmful and other dinoflagellate species in upwelling systems 1. Morphology and adaptive polymorphism. *Progress in Oceanography*, 85, 53–70.

Smayda, T.J. & Reynolds, C.S. (2001) Community assembly in marine phytoplankton: application of recent models to harmful dinoflagellate blooms. *Journal of Plankton Research*, 23, 447–461.

Smetacek, V. (1999) Diatoms and the ocean carbon cycle. *Protist*, 150, 25–32.

Smith, J., Connell, P., Evans, R.H., Gellene, A.G., Howard, M.D.A., Jones, B.H. et al. (2018) A decade and a half of *pseudo-nitzschia* spp. and domoic acid along the coast of southern California. *Harmful Algae*, 79, 87–104.

Spilling, K., Olli, K., Lehtoranta, J., Kremp, A., Tedesco, L., Tamelander, T. et al. (2018) Shifting diatom—dinoflagellate dominance during spring bloom in the Baltic Sea and its potential effects on biogeochemical cycling. *Frontiers in Marine Science*, 5, 327.

Stoeck, T., Bass, D., Nebel, M., Christen, R., Jones, M.D., Breiner, H.W., & Richards, T.A. (2010) Multiple marker parallel tag environmental DNA sequencing reveals a highly complex eukaryotic community in marine anoxic water. *Mol Ecol*, 19, 21–31.

Stoecker, D.K. (1999) Mixotrophy among dinoflagellates. *Journal of Eukaryotic Microbiology*, 46, 397–401.

Stoecker, D.K., Hansen, P.J., Caron, D.A. & Mitra, A. (2017) Mixotrophy in the marine plankton. *Annual Review of Marine Science*, 9, 311–335.

Suttle, C.A. (2007) Marine viruses — major players in the global ecosystem. *Nature Reviews. Microbiology*, 5, 801–812.

Tackmann, J., Matias Rodrigues, J.F. & von Mering, C. (2019) Rapid inference of direct interactions in large-scale ecological networks from heterogeneous microbial sequencing data. *Cell Systems*, 9, 286–296.e288.

Tatters, A.O., Schnetzer, A., Xu, K., Walworth, N.G., Fu, F., Spackeen, J.L. et al. (2018) Interactive effects of temperature, CO2 and nitrogen source on a coastal California diatom assemblage. *Journal of Plankton Research*, 40, 151–164.

Teeling, H., Fuchs, B.M., Becher, D., Klockow, C., Gardebrecht, A., Bennke, C.M. et al. (2012) Substrate-controlled succession of marine Bacterioplankton populations induced by a phytoplankton bloom. *Science*, 336, 608–611.

Tillmann, U., Hesse, K. & Tillman, A. (1999) Large-scale parasitic infection of diatoms in the Northfrisian Wadden Sea. *Journal of Sea Research*, 42, 255–261.

Trainer, V.L., Pitcher, G.C., Reguera, B. & Smayda, T.J. (2010) The distribution and impacts of harmful algal bloom species in eastern boundary upwelling systems. *Progress in Oceanography*, 85, 33–52.

Trefault, N., De la Iglesia, R., Moreno-Pino, M., Lopes dos Santos, A., Gérikas Ribeiro, C., Parada-Pozo, G. et al. (2021) Annual phytoplankton dynamics in coastal waters from Fildes Bay, Western Antarctic peninsula. *Scientific Reports*, 11, 1368.

Trombetta, T., Vidussi, F., Roques, C., Scotti, M. & Mostajir, B. (2020) Marine microbial food web networks during phytoplankton bloom and non-bloom periods: warming favors smaller organism interactions and intensifies trophic Cascade. *Frontiers in Microbiology*, 11, 11.

Utermohl, H. (1958) Zur vervollkommnung der quantitativen phytoplankton-methodik. *Mitteilungen Internationale Vereinigung fur Theoretische und Angewandte Limnologie*, 9, 1–38.

Venrick, E.L. (2012) Phytoplankton in the California current system off southern California: changes in a changing environment. *Progress in Oceanography*, 104, 46–58.

Vikebø, F.B., Strand, K.O. & Sundby, S. (2019) Wind intensity is key to phytoplankton spring bloom under climate change. *Frontiers in Marine Science*, 6, 518.

Watts, D.J., & Strogatz, S.H. (1998) Collective dynamics of 'small-world' networks. *Nature*, 393, 440-442.

Wang, H., Wei, Z., Mei, L., Gu, J., Yin, S., Faust, K. et al. (2017) Combined use of network inference tools identifies ecologically meaningful bacterial associations in a paddy soil. *Soil Biology and Biochemistry*, 105, 227–235.

Weatherdon, L.V., Magnan, A.K., Rogers, A.D., Sumaila, U.R. & Cheung, W.W.L. (2016) Observed and projected impacts of climate change on marine fisheries, aquaculture, coastal tourism, and human health: an update. *Frontiers in Marine Science*, 3, 48.

Wilson, J.M., Chamberlain, E.J., Erazo, N., Carter, M.L. & Bowman, J.S. (2021) Recurrent microbial community types driven by nearshore and seasonal processes in coastal Southern California. *Environmental Microbiology*, 23, 3225-3239.

Worden, A.Z., Follows, M.J., Giovannoni, S.J., Wilken, S., Zimmerman, A.E. & Keeling, P.J. (2015) Environmental science. Rethinking the marine carbon cycle: factoring in the multifarious lifestyles of microbes. *Science*, 347, 1257594.

Xia, L.C., Steele, J.A., Cram, J.A., Cardon, Z.G., Simmons, S.L., Vallino, J.J. et al. (2011) Extended local similarity analysis (eLSA) of microbial community and other time series data with replicates. *BMC Systems Biology*, 5(Suppl 2), S15.

Yoon, G., Gaynanova, I. & Müller, C.L. (2019) Microbial networks in SPRING - semi-parametric rank-based correlation and partial correlation estimation for quantitative microbiome data. *Frontiers in Genetics*, 10, 516.

Zhang, Y., Lin, X., Shi, X., Lin, L., Luo, H., Li, L. et al. (2019) Metatranscriptomic signatures associated with phytoplankton regime shift from diatom dominance to a dinoflagellate bloom. *Frontiers in Microbiology*, 10, 590.

SUPPORTING INFORMATION

Additional supporting information can be found online in the Supporting Information section at the end of this article.

How to cite this article: Ollison, G.A., Hu, S.K., Hopper, J.V., Stewart, B.P., Smith, J., Beatty, J.L. et al. (2022) Daily dynamics of contrasting spring algal blooms in Santa Monica Bay (central Southern California Bight). *Environmental Microbiology*, 1–19. Available from: https://doi.org/10.1111/1462-2920.16137